

# Effect of Selenium doping on the superconductivity of $\text{Nb}_2\text{Pd}(\text{S}_{1-x}\text{Se}_x)_5$

C. Q. Niu<sup>1</sup>, J. H. Yang<sup>1,\*\*</sup>, Y. K. Li<sup>1</sup>, Bin Chen<sup>2,1</sup>, N. Zhou<sup>1</sup>, J. Chen<sup>1</sup>, L. L. Jiang<sup>1</sup>, B. Chen<sup>1</sup>, X. X. Yang<sup>1</sup>, Chao Cao<sup>1</sup>, Jianhui Dai<sup>1</sup>, and Xiaofeng Xu<sup>1,\*†</sup>

<sup>1</sup>*Department of Physics and the Quantum Matter Key Laboratory of Hangzhou, Hangzhou Normal University, Hangzhou 310036, China*

<sup>2</sup>*Department of Physics, University of Shanghai for Science & Technology, Shanghai, China*

(Dated: September 18, 2018)

We study the isovalent substitution effect by partially introducing Se on S site in the newly discovered superconductor  $\text{Nb}_2\text{PdS}_5$  ( $T_c \sim 6$  K) whose upper critical field is found to be far above its Pauli paramagnetic limit. In this  $\text{Nb}_2\text{Pd}(\text{S}_{1-x}\text{Se}_x)_5$  ( $0 \leq x \leq 0.8$ ) system, superconductivity is systematically suppressed by the Se concentration and ultimately disappears when  $x \geq 0.5$ , after which a semiconducting-like ground state emerges. In spite of the considerably reduced  $T_c$  with Se doping, the ratio of the upper critical field  $H_{c2}$  to  $T_c$ , remains unaffected. Moreover, the size of the heat capacity jump at  $T_c$  is smaller than that expected for a BCS superconductor, implying that a strong-coupling theory cannot be the origin of this large upper critical field. In addition, the low-lying quasiparticle excitations are consistent with a nodeless gap opening over the Fermi surface. These results combined impose severe constraints on any theory of exotic superconductivity in this system.

A superconductor with a remarkably large upper critical field relative to its  $T_c$  always attracts sustained interest from both experimental and theoretical communities.<sup>1–4</sup> As a notable example, a very high  $H_{c2}$  observed in the iron pnictide  $\text{LaFeAsO}_{0.89}\text{F}_{0.11}$  was effectively ascribed to a two-band effect.<sup>5</sup> Theoretically, a magnetic field destroys superconductivity by two distinct mechanisms: the *orbital* effect and the Pauli paramagnetic pair-breaking effect.<sup>6</sup> In the former, the vortices penetrate into the superconductor and the associated supercurrent increases the kinetic energy of the system. When this kinetic energy gain exceeds the condensation energy, the normal state recovers. In parallel, Cooper pairs may also be broken by Zeeman splitting produced by the magnetic field coupling to the electronic spins in a spin-singlet superconductor. In weak coupling BCS theory, this Pauli limiting field  $H_p$  is  $\sim 1.84 T_c$ .<sup>7</sup> However, a growing number of superconductors are found to have  $H_{c2}$  significantly higher than the Pauli limit.<sup>8–10</sup> The excess of  $H_{c2}$  beyond the Pauli limit has been accounted for by different theories such as strong spin-orbit coupling, strong-coupling modes, multi-band effects or even spin-triplet pairing.

Very recently, a new transition metal-chalcogenide based compound  $\text{Nb}_2\text{Pd}_{0.81}\text{S}_5$  was discovered to be superconducting below  $T_c \sim 6.6$  K.<sup>11</sup> This superconductivity was found to be *unconventional* in the sense that its upper critical field, for field applied along the crystallographic *b*-axis, was reported to surpass the Pauli paramagnetic limit by a factor of 3 as  $T \rightarrow 0$  K. It was also suggested that this superconductivity may be in proxim-

ity to a magnetic instability. This very high upper critical field was tentatively ascribed to the multi-band effect or spin-triplet pairing.<sup>11,12</sup> Whilst both represent the likelihood for the enhanced  $H_{c2}$ , the experimental data are far from conclusive. Whether spin-orbit coupling or strong electron-boson coupling play a prominent role here, both of which can also elevate  $H_{c2}$ , remains to be seen. In addition, its superconducting gap symmetry, which may also provide valuable information on the pairing character (e.g. the possibility of triplet pairing), has not yet been determined.

With these questions in mind, we study the effect of Se doping in this  $\text{Nb}_2\text{Pd}(\text{S}_{1-x}\text{Se}_x)_5$  system. With the partial substitution of Se for S, the lattice parameters (and the unit cell volume) increase monotonically with Se content, indicating that a negative chemical pressure is induced. Meanwhile, the superconductivity is gradually suppressed and finally disappears around  $x=0.5$ , above which the ground state is semiconducting-like. While  $T_c$  is rather sensitive to Se doping, the reduced upper critical field,  $H_{c2}/T_c$ , is seen to be robust against impurities. Furthermore, the quasiparticle excitations are indicative of a fully gapped superconducting order parameter with weak-coupling character. Collectively, these findings shed important light on the nature of the observed superconductivity.

Polycrystalline samples of  $\text{Nb}_2\text{Pd}(\text{S}_{1-x}\text{Se}_x)_5$  with nominal Se content of  $x=0, 0.1, 0.15, 0.2, 0.25, 0.3, 0.4, 0.6$  and  $0.8$  were grown by a solid state reaction method.<sup>11</sup> The starting materials of Nb(99.99%), Pd(99.9%), and S/Se(99.99%) powders were mixed thoroughly in the ratio of 2:1:7.2 in the glove box filled with Ar gas. The excess amount of S/Se is necessary to compensate the high vapor pressure of S/Se during reaction. The pelletized mixtures were loaded into an evacuated quartz tube which was slowly heated to 825°C and kept

\*Electronic address: yjhphy@163.com

†Electronic address: xiaofeng.xu@hznu.edu.cn

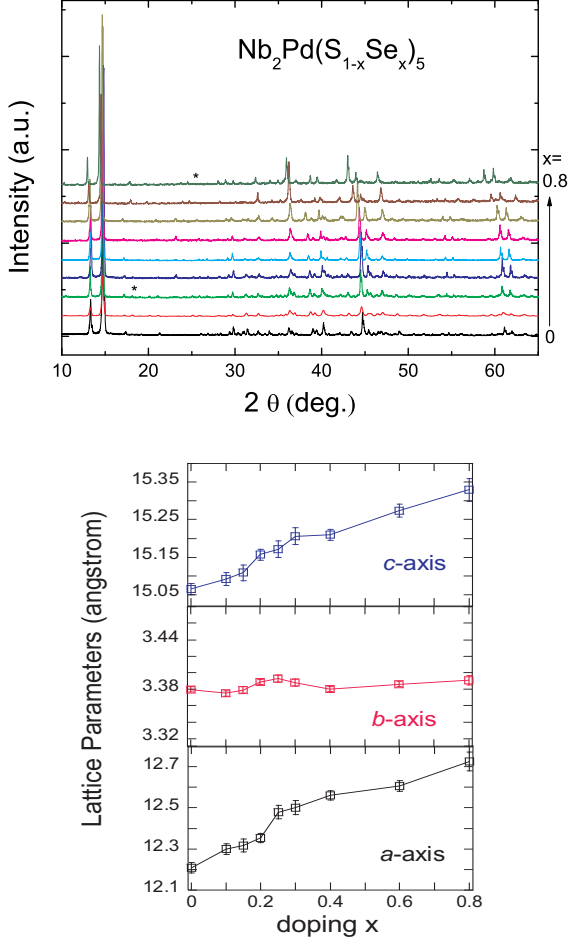


FIG. 1: (Color online) Top panel: The powder XRD patterns for a series of  $\text{Nb}_2\text{Pd}(\text{S}_{1-x}\text{Se}_x)_5$  samples studied in the paper. The asterisks mark the possible impurity phases. Bottom Panel: The lattice parameters as a function of nominal Se content extracted by using Rietveld analysis.

at this temperature for 48 hours before being quenched to room temperature. The structure of the polycrystalline samples were characterized by powder X-ray diffraction (XRD) at room temperature using a Rigaku diffractometer with  $\text{Cu } K_\alpha$  radiation and a graphite monochromator. Lattice parameters were obtained by Rietveld refinements. The resistivity of each sample was measured with a standard four-probe technique and the specific heat was measured by a long relaxation method using a commercial Quantum Design PPMS-9 system.

Figure 1(a) displays the powder XRD patterns of a series of  $\text{Nb}_2\text{Pd}(\text{S}_{1-x}\text{Se}_x)_5$  samples. The main XRD peaks of these samples can be well indexed based on a monoclinic cell structure with the  $C2/m$  space group. Extra minor peaks, marked by the asterisks in the figure, are still detectable. Indeed, the iso-structural  $\text{Nb}_2\text{PdSe}_5$  compound has been reported in previous literature.<sup>13</sup> Note that all X-ray diffractions for doped samples shift

systematically to lower  $2\theta$  angles with increasing Se concentration, implying that Se atoms are incorporated into the lattice and lead to expansion of the lattice parameters. Figure 1(b) shows how the extracted lattice parameters vary with Se content. Both the  $c$ -axis and the  $a$ -axis increase monotonically with increasing Se content, while the  $b$ -axis shows less doping dependence. Overall, these results indicate that the Se atoms are successfully doped into the system.

Figure 2(a) presents zero-field resistivity  $\rho(T)$  curves from room temperature to the lowest temperature studied for all samples, renormalized to their individual 300 K values for clarity. For the parent compound  $\text{Nb}_2\text{PdS}_5$ ,  $\rho(T)$  is metallic on cooling from room temperature and becomes superconducting below  $T_c \sim 6.3$  K. Upon Se doping, a well-defined resistivity upturn develops in the normal state at  $T_{\min}$ , which shifts to higher temperature with increasing Se content. Meanwhile,  $T_c$  is gradually suppressed by Se concentration and finally disappears as  $x \geq 0.5$ . Interestingly, the resistivity upturn can not be fitted to a gap-like excitation of  $\rho = \rho_0 \exp(E_g/k_B T)$  nor a variable-range hopping model.<sup>14,15</sup> The residual resistivity ratio is systematically reduced by Se doping. Hence, it appears more likely that this resistivity upturn results from a disorder-induced localization effect.

The magneto-transport of the superconducting samples, as exemplified for the parent compound  $\text{Nb}_2\text{PdS}_5$  shown in Fig. 2(b), was studied by fixed-field temperature sweeps. The as-determined  $H_{c2}(T)$ , using the criterion of 90% of normal state values, is summarized in Fig. 2(c). The  $H_{c2}$  for field aligned along the  $b$ -axis of  $\text{Nb}_2\text{Pd}_{0.81}\text{S}_5$  single crystal is also incorporated in the figure for comparison. As noted in the figure, whilst the  $H_{c2}$  is significantly reduced in our polycrystal compared with its single crystal profile, consistent with its highly anisotropic Fermi surface, it still exceeds the Pauli limit by a factor of  $\sim 2$ . Similar to data for single crystals of  $\text{Nb}_2\text{Pd}_{0.81}\text{S}_5$ , we also satisfactorily fitted our experimental data with the Werthamer-Helfand-Hohenberg (WHH) model.<sup>16,17</sup> This is depicted by the color-coded solid lines in Fig. 2(c).

Fig. 3 presents the detailed calorimetric study of our samples. As seen in Fig. 3(a), a clear heat capacity anomaly associated with the superconducting transition is observed at  $\sim 6$  K for the parent compound. This anomaly is seen to move to lower temperature with Se doping. In Fig. 3(b), the anomaly is isolated by subtracting the normal-state heat capacity which was fitted by  $C_n/T = \gamma_n + \beta_n T^2 + \alpha_n T^4$  (the first term represents the electronic contribution, while the remaining terms represent the phonon contribution) above  $T_c$  and extrapolated to low temperatures, as shown by the red curve.<sup>18–21</sup> Although there would be some uncertainty of the normal-state heat capacity in this method, the entropy conservation below  $T_c$  between the superconducting state and the normal state indicates that this procedure is reliable.<sup>21</sup> Here, it is worth noting that the intercept of  $C/T$  vs  $T^2$  as  $T \rightarrow 0$  K goes to zero, which indicates that the fraction of

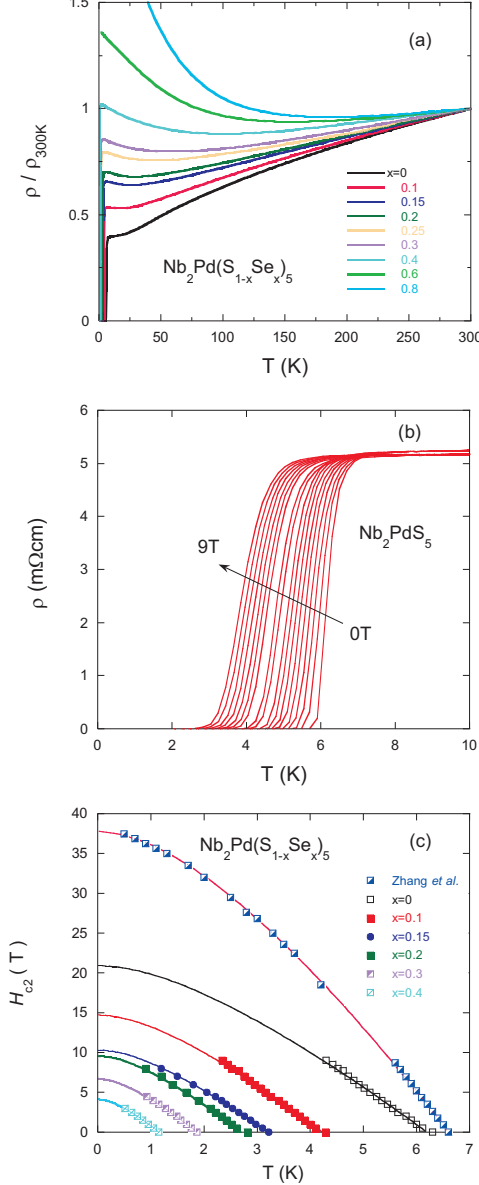


FIG. 2: (Color online) (a) Temperature dependence of the zero-field resistivity of  $\text{Nb}_2\text{Pd}(\text{S}_{1-x}\text{Se}_x)_5$  ( $0 \leq x \leq 0.8$ ). All curves are renormalized to their individual 300 K values for clarity. (b) The fixed-field temperature sweeps below  $T_c$  for  $\text{Nb}_2\text{PdS}_5$  as an example. (c) The resultant  $H_{c2}$  extracted using the criterion of 90% of normal-state resistivity. The data by Zhang *et al.* on  $\text{Nb}_2\text{Pd}_{0.81}\text{S}_5$  single crystal ( $H \parallel b$ ) were also incorporated for comparison. The solid lines represent the corresponding WHH fitting.

non-superconducting sample is indeed very small.<sup>22</sup> The resultant  $\Delta C$ , normalized to  $T$ , is plotted in Fig. 3(c).

From Fig. 3(c), the size of the heat capacity jump in our polycrystal samples is much higher than that reported in single crystal samples.<sup>11</sup> Importantly, the value of the normalized jump,  $\Delta C / \gamma_n T_c \sim 0.9$  is con-

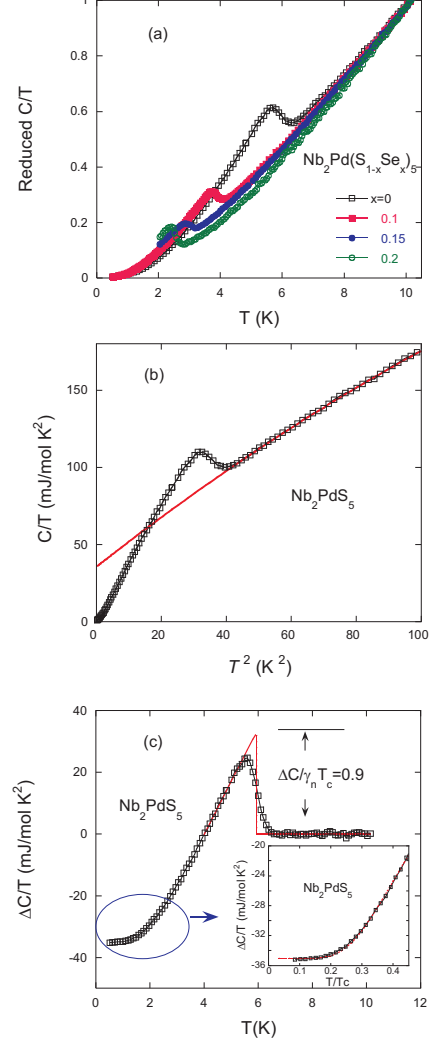


FIG. 3: (Color online) (a) Heat capacity anomalies associated with  $T_c$  for various dopings. The data are reduced to their 10 K values. (b) The plot of  $C/T$  vs  $T^2$  for  $\text{Nb}_2\text{PdS}_5$  as a demonstration. The red line stands for the fit to its normal-state heat capacity as  $C_n/T = \gamma_n + \beta_n T^2 + \alpha_n T^4$  above  $T_c$  and the extrapolation to low temperatures. The equal entropy to the superconducting state below  $T_c$  has been checked for this fitting. (c)  $\Delta C/T$  ( $= (C - C_n)/T$ ) as a function of temperature. The normalized heat capacity jump at  $T_c$ ,  $\Delta C / \gamma_n T_c$ , using the entropy conserving construction, is equal to 0.9 for  $\text{Nb}_2\text{PdS}_5$ . The inset is the blow-up of the low-temperature data enclosed in the oval of the main panel. The red line in the inset is the fit to  $\Delta C/T \sim bT^{-5/2} \exp(-\Delta_g/k_B T) - \gamma_n$ .<sup>23</sup>

siderably smaller than the weak-coupling BCS value of 1.43. The value of this normalized jump was seen to vary slightly with different doping level  $x$ , being the largest at a value of  $\sim 1.1$ . The small  $\Delta C / \gamma_n T_c$  would seem to rule out a strong-coupling origin of the observed

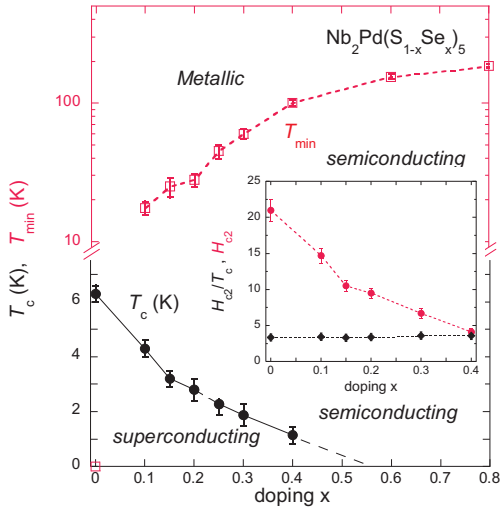


FIG. 4: (Color online) The phase diagram of  $T_c$  and resistivity minimum  $T_{\min}$  as a function of doping level  $x$ . Note that the  $y$ -axis is broken up for  $T_c$  and  $T_{\min}$ , respectively. The inset shows the evolution of  $H_{c2}$  and  $H_{c2}/T_c$  as doping.

superconductivity,<sup>24,25</sup> which was reported to be responsible for the significantly enhanced  $H_{c2}$  in the heavy fermion superconductor CeCoIn<sub>5</sub>.<sup>8</sup>

In the low temperature limit, we uncovered another interesting feature of the observed superconductivity. In a superconductor with a gap node, one expects  $C_{el} \sim T^2$  so  $\Delta C/T \sim aT - \gamma_n$ . Instead, a nodeless superconductor predicts  $\Delta C/T \sim bT^{-5/2} \exp(-\Delta_g/k_B T) - \gamma_n$ .<sup>20,22</sup> As clearly seen in the inset of Fig. 3(c), the electronic specific heat is dominated by the exponential dependence up to  $T/T_c \sim 0.45$ , indicating a nodeless gap on the Fermi surface. This seemingly precludes a  $d$ -wave gap or a simple  $p_x(p_y)$  symmetry where node(s) are present, although complex order parameter structures such as  $p_x + ip_y$  are still possible.

Finally, the resultant phase diagram is summarized in Fig. 4. Accompanied by an increase of resistivity minimum  $T_{\min}$ , the superconducting transition  $T_c$  is systematically suppressed by Se doping in Nb<sub>2</sub>Pd(S<sub>1-x</sub>Se<sub>x</sub>)<sub>5</sub>, and ultimately disappears when  $x \geq 0.5$ , where the ground state is semiconducting-like, presumably induced by disorder effect. Intriguingly, as seen in the inset, while the upper critical field  $H_{c2}$  is significantly reduced by the doping, the normalized  $H_{c2}/T_c$  is rather robust against impurities, exceeding the Pauli limiting value of  $1.84T_c$  by a factor of 2. The robustness of this large  $H_{c2}$  relative to  $T_c$  up to  $x \sim 0.4$  seems at odds with the spin triplet origin of the enormous  $H_{c2}$  observed in Nb<sub>2</sub>Pd<sub>0.81</sub>S<sub>5</sub>, which should be sensitive to non-magnetic impurity scattering. To firmly rule out the spin triplet scenario, it would be a litmus test to study the Knight shift suppression below  $T_c$ .<sup>26,27</sup>

In summary, we study the isovalent doping effect, i.e., the partial substitution of Se for S, in the newly discovered superconducting Nb<sub>2</sub>PdS<sub>5</sub> system. While  $T_c$  substantially decreases with Se doping, its high  $H_{c2}$  with respect to  $T_c$ ,  $H_{c2}/T_c$ , is found to be immune to the Se impurities. Moreover, the heat capacity study reveals that the superconductivity is fully gapped, with relatively weak-coupling strength. Both of these findings seemingly argue against strong-coupling and spin-triplet pairing as the origin of the large  $H_{c2}$ . Alternatively, multi-band effects or strong spin-orbit coupling or even a subtle combination of the two, could be responsible for the large  $H_{c2}$ . Regarding the latter, it shall be very instructive to substitute heavier elements, such as Pt, for Pd to study the role of spin-orbit coupling in this exotic superconductor.

The authors would like to thank N. E. Hussey, A. F. Bangura, C. M. J. Andrew, E. A. Yelland, Wenhe Jiao, Guanghan Cao, Zhuan Xu, Xiaofeng Jin for stimulating discussions and Q. L. Ye, H. D. Wang for collaborative support. The work is sponsored by the National Natural Science Foundation of China.

- <sup>1</sup> P. A. Lee, N. Nagaosa, X. G. Wen, Rev. Mod. Phys. **78**, 17 (2006).
- <sup>2</sup> H. Lei *et al.*, Phys. Rev. B **85**, 094515 (2012).
- <sup>3</sup> H. Q. Yuan *et al.*, Nature **457**, 565568 (2009).
- <sup>4</sup> K. Okuda, M. Kitagawa, T. Sakakibara, and M. Date, J. Phys. Soc. Jpn. **48**, 21572158 (1980).
- <sup>5</sup> F. Hunte, J. Jaroszynski, A. Gurevich, D. C. Larbalestier, R. Jin, A. S. Sefat, M. A. McGuire, B. C. Sales, D. K. Christen, D. Mandrus, Nature **453**, 903 (2008).
- <sup>6</sup> S. Uji, H. Shinagawa, T. Terashima, T. Yakabe, Y. Terai, M. Tokumoto, A. Kobayashi, H. Tanaka, and H. Kobayashi, Nature **410**, 908 (2001).
- <sup>7</sup> F. Zuo, J. S. Brooks, R. H. McKenzie, J. A. Schlueter, and J. M. Williams, Phys. Rev. B **61**, 750 (2000).
- <sup>8</sup> Y. Mizukami, H. Shishido, T. Shibauchi, M. Shimozawa, S. Yasumoto, D. Watanabe, M. Yamashita, H. Ikeda, T.

- Terashima, H. Kontani and Y. Matsuda, Nat. Phys. **7**, 849 (2011).
- <sup>9</sup> I. J. Lee, P. M. Chaikin, and M. J. Naughton, Phys. Rev. B **62**, 14669 (2000).
- <sup>10</sup> J.-F. Mercure, A. F. Bangura, Xiaofeng Xu, N. Wakeham, A. Carrington, P. Walmsley, M. Greenblatt, and N. E. Hussey, Phys. Rev. Lett. **108**, 187003 (2012).
- <sup>11</sup> Q. Zhang, G. Li, D. Rhodes, A. Kiswandhi, T. Besara, B. Zeng, J. Sun, T. Siegrist, M. D. Johannes and L. Balicas, Sci. Rep. **3**, 1446 (2013).
- <sup>12</sup> Q. Zhang, D. Rhodes, B. Zeng, T. Besara, T. Siegrist, M. D. Johannes, L. Balicas, arXiv:1306.6868.
- <sup>13</sup> D. A. Keszler, J. A. Ibers, Maoyu Shang and Jiaxi Lu, J. Solid State Chem. **57**, 68 (1985).
- <sup>14</sup> Xiaofeng Xu, A. F. Bangura, J. G. Analytis, J. D. Fletcher, M. M. J. French, N. Shannon, J. He, S. Zhang, D. Mandrus,

- R. Jin, and N. E. Hussey, Phys. Rev. Lett. **102**, 206602 (2009)
- <sup>15</sup> Ashcroft and Mermin, Solid State Physics (Cornell University Press, Cornell, 1975).
- <sup>16</sup> N. R. Werthamer, E. Helfand, P. C. Hohenberg Phys. Rev. **147**, 295 (1966).
- <sup>17</sup> Xiaofeng Xu *et al.*, Phys. Rev. B **87**, 224507 (2013).
- <sup>18</sup> Y. Nakajima, T. Nakagawa, T. Tamegai, and H. Harima, Phys. Rev. Lett. **100**, 157001 (2008).
- <sup>19</sup> Y. Nakajima, H. Hidaka, T. Nakagawa, T. Tamegai, T. Nishizaki, T. Sasaki, and N. Kobayashi, Phys. Rev. B **85**, 174524 (2012).
- <sup>20</sup> O. J. Taylor, A. Carrington, J. A. Schlueter, Phys. Rev. Lett. **99**, 057001 (2007).
- <sup>21</sup> P. Walmsley *et al.* Phys. Rev. Lett. **110**, 257002 (2013).
- <sup>22</sup> N. E. Hussey, Adv. Phys. **51**, 1685 (2002).
- <sup>23</sup> Note that the free parameters in this fitting are  $b$  and  $\Delta_g$  only.  $\gamma_n$  is fixed to be the one extracted from Fig. 3(b). The resulting  $\Delta_g$  value is  $\sim 1.9k_B T_c$ , close to the weak-coupling BCS value of  $1.76k_B T_c$ , further indicating that the coupling strength is not strong in this system.
- <sup>24</sup> J. P. Carbotte, Rev. Mod. Phys. **62**, 1027 (1990).
- <sup>25</sup> P. Popovich, A. V. Boris, O. V. Dolgov, A. A. Golubov, D. L. Sun, C. T. Lin, R. K. Kremer, and B. Keimer, Phys. Rev. Lett. **105**, 027003 (2010).
- <sup>26</sup> S. Raghu, A. Kapitulnik, and S. A. Kivelson, Phys. Rev. Lett. **105**, 136401 (2010).
- <sup>27</sup> I. J. Lee, S. E. Brown, W. G. Clark, M. J. Strouse, M. J. Naughton, W. Kang, and P. M. Chaikin, Phys. Rev. Lett. **88**, 017004 (2001).